Supplemental Figure Legends

Figure S1. EGF-induced internalization of E-cad into Cav1-coated endocytic structures is observed in both normal and neoplastic epithelial cells.

(a-d') Fluorescence micrographs of cultured epithelial cells stained for E-cad (green) and Cav1 (red). Normal epithelial cells (MDCK cells a, a') were stimulated with EGF (30 ng/ml) for one hour while pancreatic tumor cells were fixed under resting conditions (BxPC-3 b, b'; PANC-1 c, c'; HPAF-II d, d'). Insets represent low magnification images of the corresponding higher magnification images. All cells show a marked formation of E-cad-containing endocytic structures surrounded by Cav1 (arrows).

Figure S2 and Supplemental Movies 1 and 2. Live cell imaging of EGF induced internalization of E-cad within caveolin coated structures. PANC1 cells co-expressing E-cad-GFP and Cav1-DsRed were serum starved for four hours prior to stimulation with 100ng/mL EGF**.** Subsequent to stimulation with EGF for one hour, dual color time-lapse microscopy was performed. (a, b) Ecad-GFP and Cav1-DsRed proteins were visualized in a pair of PANC1 cells displaying invaginations of the cell border following stimulation with EGF for one hour. Both proteins are found to overlap within these invaginations emanating from the cell border (c). (a'-c') Still images collected from a timelapse series of scans of the boxed region shown in (a-c). Arrows denote vesicle budding from the border invagination that contains both Ecad-GFP and Cav1-DsRed protein. (d-d"') A similar series of still images taken from a timelapse series of another

additional PANC1 cell showing a tubule extending from a cell-cell border that contains both Ecad-GFP and Cav1-DsRed. The active budding of vesicles bearing both E-cad and Cav1 proteins is observed. (Movies 1 and 2) Correlating timelapse captures for the still images seen in (a-d''').

Figure S3/Movie S3. 3D-reconstruction of Cav1-coated endosomes in HPAF-II pancreatic tumor cells. Cultured HPAF-II cells were serum-starved followed by stimulation for 20 minutes with EGF. Subsequently, cells were fixed, stained for E-cad (green) and Cav1 (red), and imaged using an LSM510 confocal microscope, acquiring images at 3 μm intervals (at least 23 slices). 3D reconstruction was performed using LSM510 software. The EGF-induced endocytic structures contain E-cad and are surrounded by Cav1. Rotation of the 3D image (movie 3) shows the intracellular localization of these structures.

Figure S4. Stable expression of Cav1 WT-GFP or mutant Cav1Y-14F-GFP does not alter EGF-based cytoplasmic signaling cascades. Western blot analysis of HPAF-II cells stably expressing either WT or mutant (Y14F) Cav1-GFP that were stimulated with 100 ng/ml of EGF for 15 minutes. Blots were probed with antibodies to phospho-specific, active forms of c-Src and Erk kinase as well as GFP, Src, Erk, actin and γ-tubulin for loading controls. **a,** After EGF stimulation (100 ng/ml for 15 min) the phospho-Erk levels increased up to 3 fold in the GFP vector, WT and mutant Cav-1-GFP expressing cell lines. **b,** Densitometry was performed and the relative level of phospho-Erk (pErk) to total Erk protein is displayed for each of the stable HPAF cell lines. Data represent

the average from three separate experiments. Error bars represent standard error. **c,** An identical analysis was done for the relative levels of active Src (pSrc) in the GFP, WT and mutant Cav-1-GFP stable HPAF cells. Appreciable differences in active Src levels were not seen following stimulation with 100 ng/ml of EGF for 15 minutes. **d,** Relative changes in pSrc levels were analyzed through densitometry and the values reported represent the average from three experiments with error bars denoting the standard error.

Figure S5. Expression of wt Cav1 or Cav1Y14D phospho-mimetic protein increase caveolae number and the formation of internalized caveosome-like structures containing E-Cad. Electron micrographs of NRK cells transiently expressing GFP tagged versions of (a, a') WTCav1 (b, b') Cav1Y14F and (c, c') Cav1Y14D. Gold particle labeling with enhanced anti-GFP antibody methods was performed for detection of the expressed Cav1 protein. Note the large increase in caveolae number in the Cav1wt (a-a') or Cav1Y14D (c,c') expressing cells compared to the Cav1Y14F expressing cells (b,b'). (d) Quantitative comparison of caveolae witih obvious attachments to the plasma membrane (d) or found in clusters with no obvious proximity to the cell surface (e). Data represent the average number of caveolae structures for each mm of cytoplasm/membrane examined in 30 cells for each treatment group. Scale bar =400nm (f) Frequency of PANC1 cells with internal large caveolin/Ecad clusters, similar to those observed in Figs 2 and S1, following the transient expression of GFP tagged versions of WTCav1 and the Cav1Y14F, Cav1Y14D

mutants. The number of “caveosome-like” structures is markedly increased in the Cav1Y14D expressing cells which is consistent with the EM observations and the premise that Src-mediated phosphoylation of Cav1 stimulates cavesome formatation.

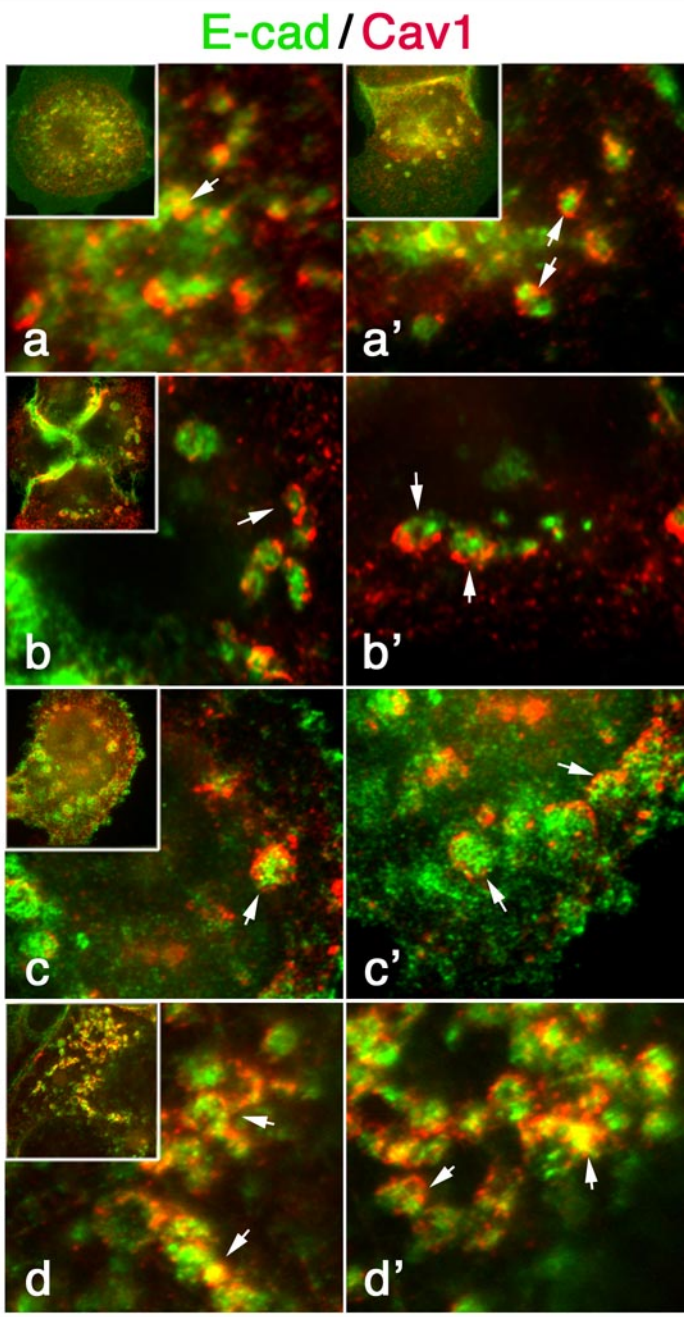

Fig. S1

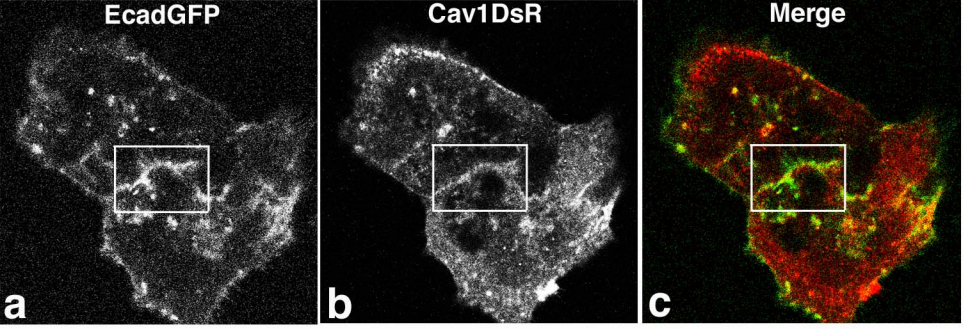
EcadGFP
Cav1DsR
Merge
a
b
c

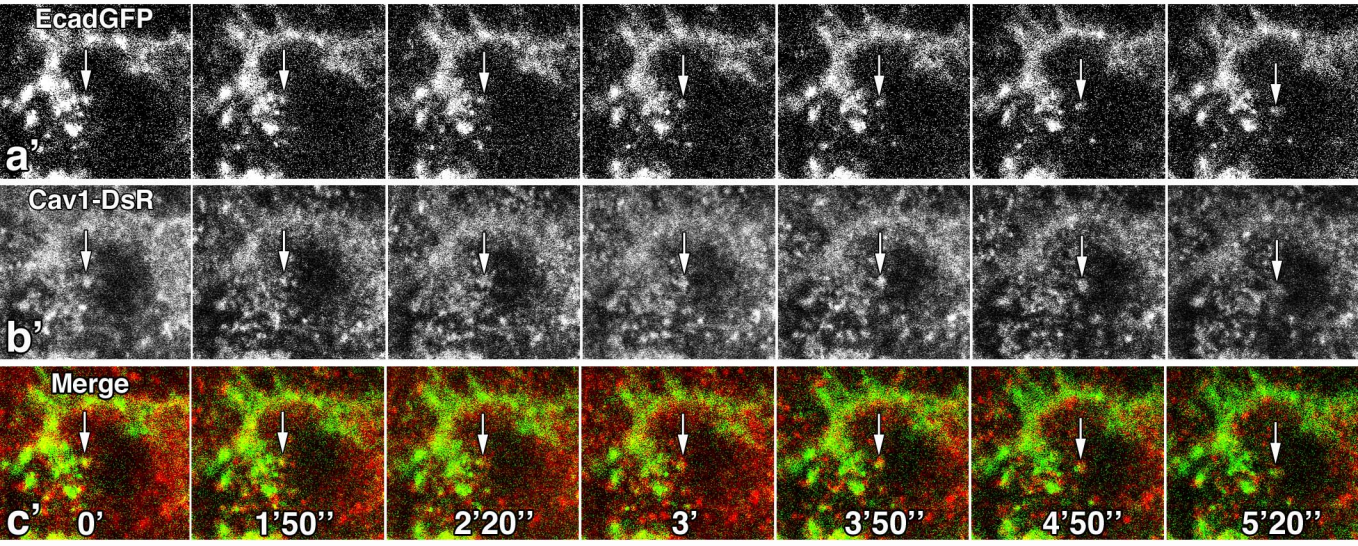
EcadGFP
a'
Cav1-DsR
b'
Merge
c'
0'
1'50''
2'20''
3'
3'50''
4'50''
5'20''

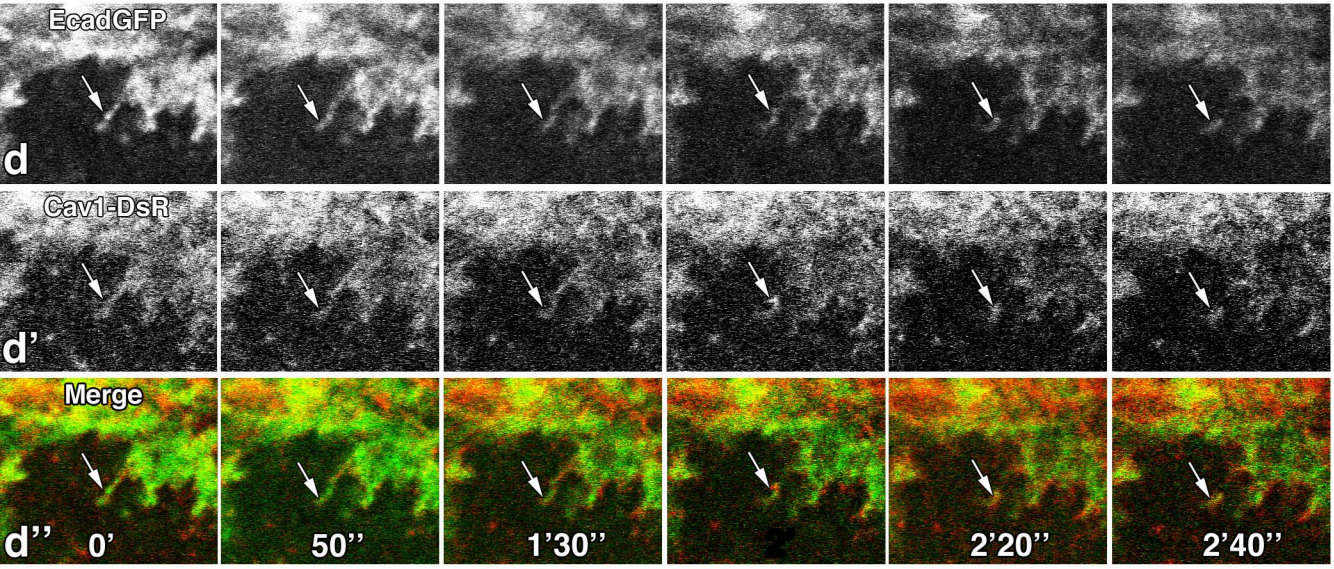
EcadGFP
d
Cav1-DsR
d'
Merge
d''
0'
50''
1'30''
2'
2'20''
2'40''

Fig. S2

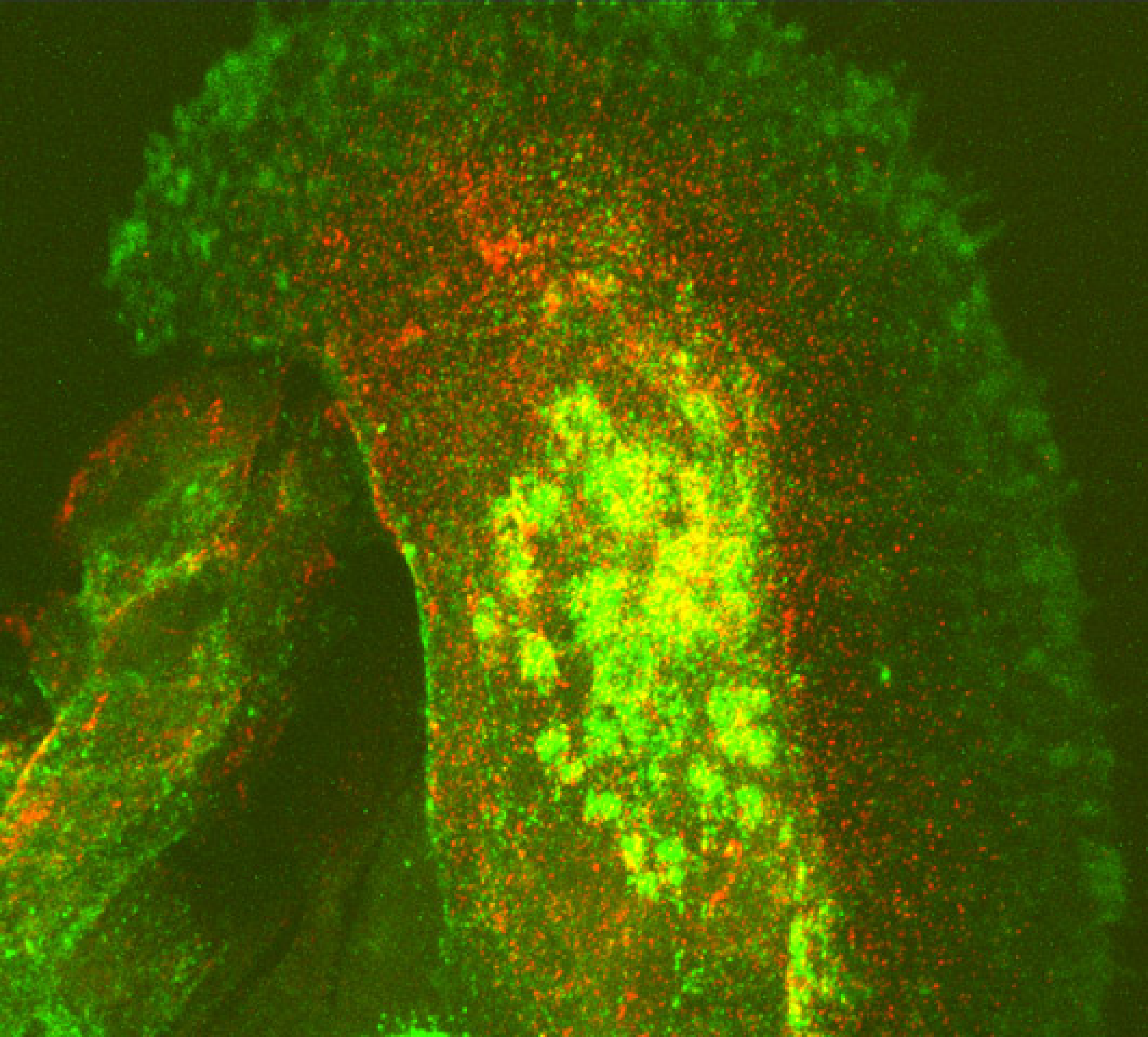

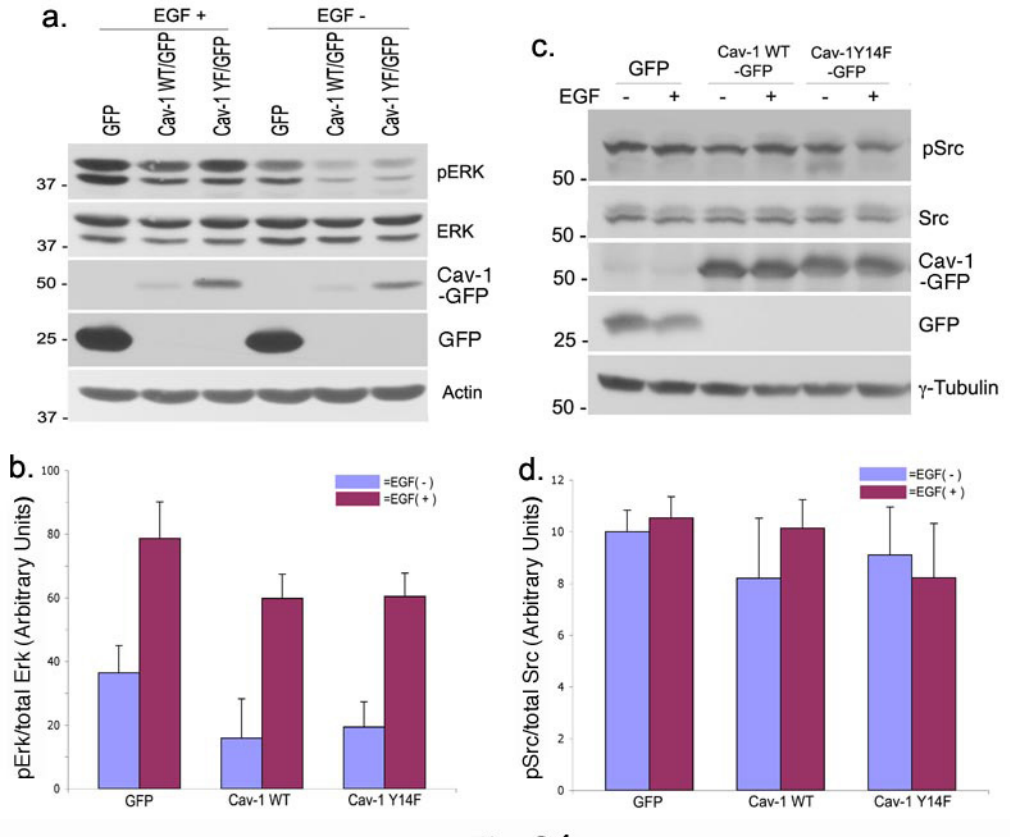
a.
EGF +
EGF -
GFP
Cav-1 WT/GFP
Cav-1 YF/GFP
GFP
Cav-1 WT/GFP
Cav-1 YF/GFP
37
pERK
37
ERK
50
Cav-1 -GFP
25
GFP
Actin
37
c.
GFP
Cav-1 WT -GFP
Cav-1Y14F -GFP
EGF - + - + - +
50
pSrc
50
Src
50
Cav-1 -GFP
25
GFP
50
γ-Tubulin
b.
=EGF(-)
=EGF(+)
pErk/total Erk (Arbitrary Units)
100
80
60
40
20
0
GFP
Cav-1 WT
Cav-1 Y14F
d.
=EGF(-)
=EGF(+)
pSrc/total Src (Arbitrary Units)
12
10
8
6
4
2
0
GFP
Cav-1 WT
Cav-1 Y14F

Fig. S4

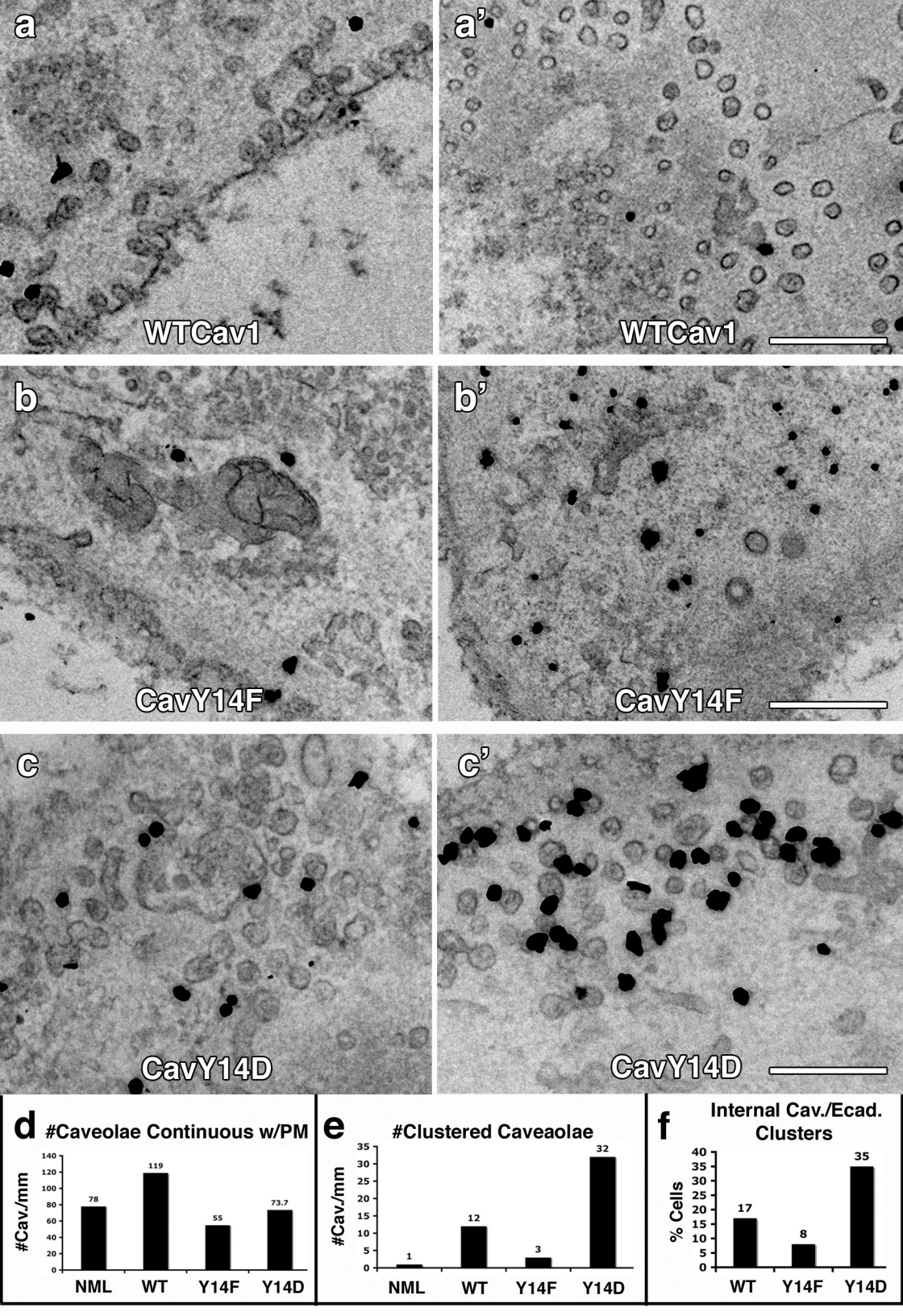
a
WTCav1
a'
WTCav1
b
CavY14F
b'
CavY14F
c
CavY14D
c'
CavY14D
d
#Caveolae Continuous w/PM
#Cav./mm
140
120
100
80
60
40
20
0
78
119
55
73.7
NML
WT
Y14F
Y14D
e
#Clustered Caveaolae
#Cav./mm
35
30
25
20
15
10
5
0
1
12
3
32
NML
WT
Y14F
Y14D
f
Internal Cav./Ecad. Clusters
% Cells
40
35
30
25
20
15
10
5
0
17
8
35
WT
Y14F
Y14D

Fig. S5